

Synthesis of MgO-SiO₂ Amorphous Silicate Nanoparticles by Induction Thermal Plasmas

誘導結合型熱プラズマによるMgO-SiO₂系非晶質ケイ酸塩ナノ粒子の合成

Masahito Yagishita, Sooseok Choi, Takayuki Watanabe, Junya Matsuno, Akira Tsuchiyama
八木下将史, 崔 秀錫, 渡辺隆行, 松野淳也, 土山 明

1) Department of Environmental Chemistry and Engineering, Tokyo Institute of Technology
4259 G1-22, Nagatsuta, Yokohama, Kanagawa 226-8502, Japan

東京工業大学大学院総合理工学研究科 〒226-8502 横浜市緑区長津田町4259番地G1-22

2) Department of Earth and Space Science, Graduate School of Science, Osaka University
1-1 Machikaneyama, Toyonaka, Osaka 556-0043, Japan

大阪大学大学院理学研究科 〒556-0043 豊中市待兼山町1-1

Crystalline silicate found in circumstellar regions and in primitive materials of the solar system is believed to be crystallized from amorphous silicates like as GEMS (glass with embedded metal and sulfides). MgO-SiO₂ amorphous silicate and iron embedded MgO-SiO₂ amorphous silicate nanoparticles were successfully prepared by induction thermal plasmas (ITP) in order to obtain GEMS analogue materials for alteration experiment. The morphology of synthesized analogue particles is very similar to GEMS. Si/Mg fractionation was found in the ITP process of synthesis of MgO-SiO₂ silicate nanoparticles due to the different nucleation temperatures of Mg and Si.

1. Introduction

Crystalline silicate in circumstellar regions and in primitive materials of the solar system is believed to be crystallized from amorphous silicates. One candidate material of such amorphous material is GEMS (glass with embedded metal and sulfide), which generally exists in cometary dust [1,2]. According to recent work, it is composed of amorphous silicate including iron metal in the size of few tens of nanometer. In order to reveal the evolution of amorphous silicate in the early solar system, the alteration experiment is required.

In this study, we aim to synthesize analogue material of GEMS which is iron embedded MgO-SiO₂ amorphous silicate by ITP (induction thermal plasmas). ITP provides high temperature environment with rapid quenching. Therefore, all introduced materials are immediately evaporated and subsequently form metastable state nanoparticles. Since synthesis of amorphous silicate with two elements by ITP is not well understood, preparation of MgO-SiO₂ amorphous silicate nanoparticles was carried out at first. Then, synthesis of iron embedded sample on GEMS mean composition [3] was followed.

2. Experimental

Fig.1 shows experimental setup composed of the RF torch and the synthesis chamber, used for amorphous silicate nanoparticles preparation. Precursor is injected from the powder feeder by Ar

carrier gas. Its feeding rate was fixed at 250 mg/min. SiO₂ (quartz), MgO, and Fe powders in the average size of 4μm, were physical mixed and used as the precursor. Synthesized nanoparticles were collected on the chamber wall after the plasma treatment.

Table 1 shows experimental condition for the synthesis system. Ar-O₂ (oxidative) sheath gas and Ar-He (inert) sheath gas are used for MgO-SiO₂ sample and iron embedded sample, respectively.

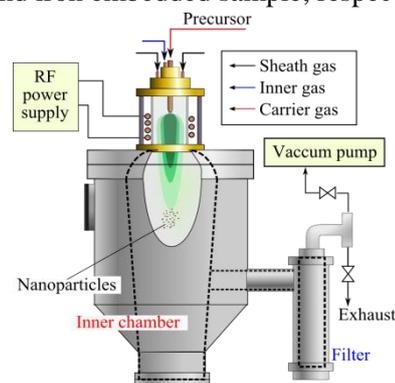


Fig.1. Experimental setup.

Table 1. Experimental conditions.

	Magnesia silicate	GEMS
Sheath gas	Ar-O ₂ , 60+5 slpm	Ar-He, 60+5 slpm
Inner gas	Ar, 5 slpm	
Carrier gas	Ar, 4-6.5 slpm	
Composition	Mg/Si = 0.17-0.64	Mg/Si, Fe/Si = 0.65, 0.56
Starting materials	SiO ₂ (quartz), MgO	Fe, SiO ₂ (quartz), MgO
Average size	4μm	
Feeding rate	250 mg/min	
Plasma power plate	30 kW	
Frequency	4 MHz	
Pressure	760 Torr	

3. Results and discussion

Fig.2 shows XRD patterns of MgO-SiO₂ amorphous silicate nanoparticles which were synthesized under oxidative plasma sheath gas condition. Although forsterite peaks are observed in the high MgO contents of 40 wt.% and 50 wt.% in the precursor, amorphous materials are successfully synthesized in low MgO contents.

Table 2 shows MgO contents and Mg/Si ratio in the precursor and in the final product measured by ICP-AES. Reduced Mg content in final products indicates the fractionation of Mg and Si in the plasma treatment. The fractionation is regarded to occur in condensation stage due to the different nucleation temperatures of Mg and Si.

Fig.3 shows XRD results of synthesized iron metal embedded MgO-SiO₂ silicate nanoparticles under inert sheath gas condition. In the Fig.3, peaks corresponding to iron metal and halo pattern for amorphous phase are clearly measured while iron oxides and minerals are not observed. Iron exists as metal during Mg and Si are oxidized due to its higher Gibbs free energy of oxidation than Si and Mg.

Fig.4 shows TEM images of (a) synthesized MgO-SiO₂ silicate particles (MgO 30 wt.%), (b) synthesized iron metal embedded MgO-SiO₂ silicate particles, (c) magnification of the GEMS analogue, and (d) GEMS grain in the interplanetary dust particles [3]. From Fig.4 (a) it is found that the synthesized MgO-SiO₂ silicate particles (MgO 30 wt.%) are amorphous with sub-micron size. Morphology of the prepared iron embedded nanoparticle in Fig.4 (b) and (c) is very similar to GEMS in sizes of amorphous particle and included iron metal. EDS semi- quantitative analysis result of the Mg/Si change from 0.56 to 0.43 is the same trend with ICP-AES measurement. Still, further investigations on reaction of raw material in ITP are needed to understand the synthesis mechanism.

4. Conclusion

GEMS analogue material was obtained by using ITP method which has high temperature and rapid quenching. Further investigation for the synthetic mechanism for Mg and Si is required to understand the whole process of iron metal embedded MgO-SiO₂ silicate nanoparticles.

Table 2 Chemical analysis on precursor and final product

Starting material		Synthesized powder
MgO [wt. %]	Mg/Si [-]	Mg/Si [-]
10	0.17	0.14
20	0.37	0.22
30	0.64	0.30

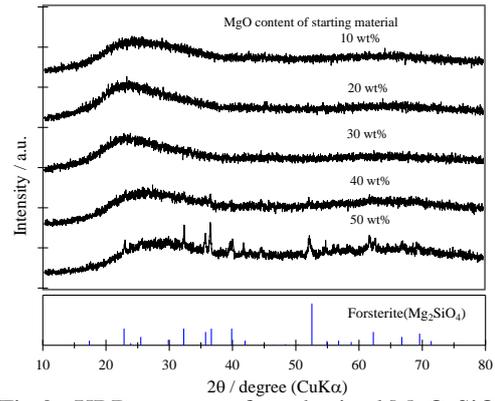


Fig.2. XRD patterns of synthesized MgO-SiO₂ amorphous silicate powder.

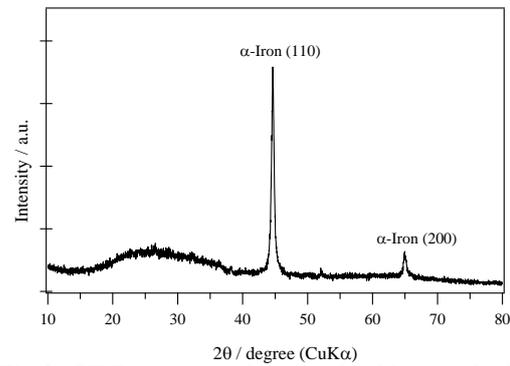


Fig.3. XRD patterns of synthesized iron embedded MgO-SiO₂ amorphous silicate powder.

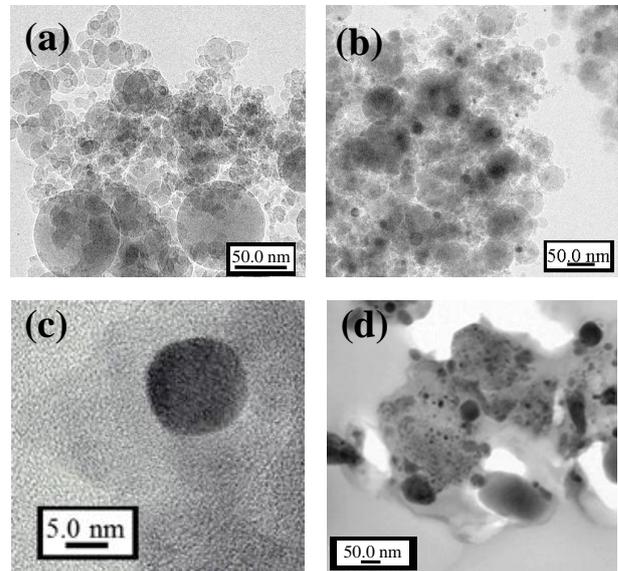


Fig.4. TEM image of synthesized materials and GEMS: (a) MgO-SiO₂ (30 wt%), (b) GEMS analogue, (c) magnification of analogue, and (d) GEMS in the interplanetary dust particles.

5. Reference

- [1] F. Kemper, W.J. Vriend, and A.G.G.M. Tielens: *Astrophys. J.* **609** (2004) 826.
- [2] J.P. Bradley: *Science* **265** (1994) 925.
- [3] L.P. Keller, S. Messenger: *Geochim. Cosmochim. Acta* **75** (2011) 5336.